Bredow, E., Steinberger, B. (2018): Variable Melt Production Rate of the Kerguelen HotSpot Due To Long-Term Plume-Ridge Interaction. - *Geophysical Research Letters*, *45*, 1, pp. 126—136.

DOI: http://doi.org/10.1002/2017GL075822

AGU PUBLICATIONS

Geophysical Research Letters

RESEARCH LETTER
10.1002/2017GL075822

Key Points:
- Constant plume influx can result in variable melt production rate due to plume-ridge interaction
- Ninetyeast Ridge has been created by on-ridge volcanism, with plume material from below the Australian plate
- Amsterdam-Saint Paul Plateau has been generated by plume material flowing toward the Southeast Indian Ridge

Supporting Information:
- Supporting Information S1
- Data Set S1

Correspondence to:
E. Bredow,
eva.bredow@gfz-potsdam.de

Citation:
Bredow, E., & Steinberger, B. (2018). Variable melt production rate of the Kerguelen hotspot due to long-term plume-ridge interaction. *Geophysical Research Letters*, *45*, 126–136. https://doi.org/10.1002/2017GL075822

Received 26 SEP 2017
Accepted 6 DEC 2017
Accepted article online 12 DEC 2017
Published online 8 JAN 2018

Variable Melt Production Rate of the Kerguelen HotSpot Due To Long-Term Plume-Ridge Interaction

Eva Bredow[1] **and Bernhard Steinberger**[1,2]

[1]GFZ German Research Centre for Geosciences, Potsdam, Germany, [2]Centre for Earth Evolution and Dynamics, University of Oslo, Oslo, Norway

Abstract For at least 120 Myr, the Kerguelen plume has distributed enormous amounts of magmatic rocks over various igneous provinces between India, Australia, and Antarctica. Previous attempts to reconstruct the complex history of this plume have revealed several characteristics that are inconsistent with properties typically associated with plumes. To explore the geodynamic behavior of the Kerguelen hotspot, and in particular address these inconsistencies, we set up a regional viscous flow model with the mantle convection code ASPECT. Our model features complex time-dependent boundary conditions in order to explicitly simulate the surrounding conditions of the Kerguelen plume. We show that a constant plume influx can result in a variable magma production rate if the plume interacts with nearby spreading ridges and that a dismembered plume, multiple plumes, or solitary waves in the plume conduit are not required to explain the fluctuating magma output and other unusual characteristics attributed to the Kerguelen hotspot.

1. Introduction

The basaltic rocks produced by the Kerguelen mantle plume record at least 120 Ma of persistent volcanic activities and yield altogether an estimated volume of approximately 2.5×10^7 km^3 (Coffin et al., 2002). These tremendous amounts include the Kerguelen Plateau in the southern Indian Ocean, which is the second largest oceanic plateau worldwide (Coffin & Eldholm, 1994) and the Ninetyeast Ridge, extended almost parallel to the 90th meridian east over a length of more than 5,000 km and thus the longest linear tectonic feature on Earth (Duncan & Richards, 1991; Mahoney et al., 1983) (Figure 1). Reconstructing the long-term geodynamic history of the Kerguelen hotspot is, however, not as straightforward as assigning the Kerguelen Plateau to the classically expected giant eruptions of an impacting plume head and the Ninetyeast Ridge to the continuous surface expression of a stable plume tail (Richards et al., 1989).

Instead, the plume started to affect the surface of the Earth rather unconventionally with a number of small-volume magmatic provinces that were placed on the contiguous continental crust of eastern Gondwana. The earliest magmatism that recent studies have associated with the Kerguelen plume began during the Early Cretaceous in the Comei area, presently located in southeastern Tibet (145–130 Ma; Liu et al., 2015; Zhu et al., 2008, 2009), followed by several distinct eruption phases of the Bunbury Basalts in southwest Australia (between 137 and 123 Ma; Coffin et al., 2002; Frey et al., 1996; Olierook et al., 2016).

After the continental breakup of India and Antarctica around 132–130 Ma (Gaina et al., 2007; Müller et al., 2016; Powell et al., 1988), the Indian Ocean started to open and dispersed continental material, in particular several microcontinents, throughout the growing ocean basin. Evidence for continental material has been found at the Naturaliste Plateau, the Wallaby Plateau, the Zenith Plateau, the Batavia Knoll and the Gulden Draak Knoll (all of which are submarine plateaus currently positioned off the west coast of Australia) (Direen et al., 2017; Gardner et al., 2015; Whittaker et al., 2016), at several parts of the Southern Kerguelen Plateau (Coffin et al., 2002) and at Elan Bank (located northwest of the Southern Kerguelen Plateau) (Borissova et al., 2003; Frey et al., 2000; Gaina et al., 2003; Ingle et al., 2002; Nicolaysen et al., 2001; Weis et al., 2001). Subsequently, large parts of these continental fragments were overlain by plume material. Age determinations of recovered igneous rocks revealed ~130–125 Ma at the Naturaliste Plateau (Direen et al., 2017; Olierook et al., 2017), ~124 Ma at the Wallaby Plateau (Olierook et al., 2015), and 117 Ma at the Gulden Draak Knoll (Whittaker et al., 2016). Further evidence of plume activities at ≤126 Ma are provided by the Seaward Dipping Reflectors abutting the Southern Kerguelen Plateau (Stagg et al., 2006).

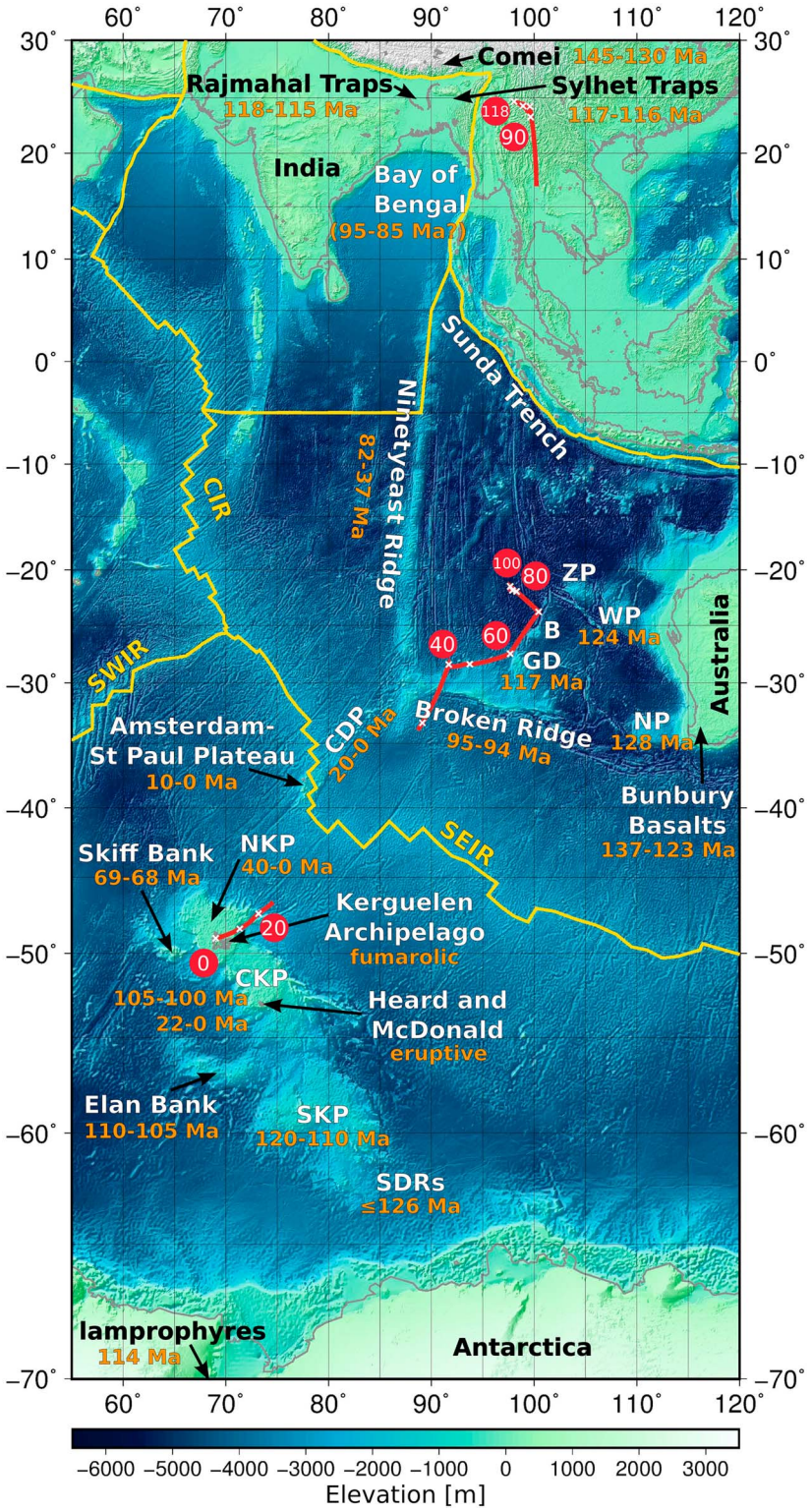

Figure 1. Topographic map of the Indian Ocean and the surrounding continents showing an overview of the igneous provinces, which are mostly attributed to the Kerguelen plume. Age estimates are labeled in orange (see text for references). The red line shows the predicted hotspot track, distributed over several plates and with plume positions (in Ma); plate boundaries are shown as yellow lines. NKP, CKP, SKP = Northern, Central, and Southern Kerguelen Plateau, respectively; NP, WP, ZP = Naturaliste, Wallaby, and Zenith Plateau, respectively; B = Batavia Knoll; GD = Gulden Draak Knoll; SEIR, SWIR, CIR = Southeast, Southwest, and Central Indian Ridge, respectively; CDP = Chain of the Dead Poets; SDRs = Seaward Dipping Reflectors.

The first larger volumes of volcanic material, considered as the actual Large Igneous Province (LIP) of the Kerguelen Plume, shaped the Southern Kerguelen Plateau in the growing basin of the Indian Ocean between 120 and 110 Ma (Coffin et al., 2002; Duncan, 2002). Thus, the LIP postdated the continental breakup by approximately 10 Ma, although older igneous rocks might be concealed at greater depths than penetrated by previous drilling campaigns. Parallel to the development of the Southern Kerguelen Plateau, further small-scale volcanism created the Rajmahal Traps (118–115 Ma; Baksi, 1995; Coffin et al., 2002; Kent et al., 2002) and Sylhet Traps (118–116 Ma; Ghatak & Basu, 2011; Ray et al., 2005) on the Indian continental margin and lamprophyre dikes on the conjugate Antarctic margin (114 Ma Coffin et al., 2002), whereas the Elan Bank microcontinent was capped by plume material between 110 and 105 Ma (Coffin et al., 2002; Duncan, 2002).

In contrast to the classically predicted short pulse of vigorous magmatic activity lasting only a few million years (e.g., Bryan & Ernst, 2008; Coffin & Eldholm, 1994), the large-volume magma production of the Kerguelen plume continued for a much longer period and resulted in the formation of the Central Kerguelen Plateau between 105 and 100 Ma (Coffin et al., 2002; Duncan, 2002) and the (at that time) contiguous Broken Ridge between 100 and 95 Ma (Coffin et al., 2002; Duncan, 2002), both of which are generally also considered as part of the Kerguelen LIP.

Afterward, the plume productivity decreased (Coffin et al., 2002) and created the Ninetyeast Ridge, probably starting around 95 Ma, although the northernmost part is currently covered by the thick sediment load of the Bengal Fan (Coffin et al., 2002). The observable part of the Ninetyeast Ridge is explicitly age-progressive and ranges in age approximately from 82 to 37 Ma (Coffin et al., 2002; Duncan, 1991). Its clear, linear structure has been attributed to the rapid northward motion of the Indian Plate over the Kerguelen plume by many previous studies (e.g., Duncan & Richards, 1991; Mahoney et al., 1983). Evidence for small-scale plume activity on the Antarctic plate in this period was found at Skiff Bank (69–68 Ma; Coffin et al., 2002; Duncan, 2002).

The separation of the Kerguelen Plateau and the Broken Ridge was initiated by the onset of seafloor spreading at the Southeast Indian Ridge around 40 Ma (Müller et al., 2016; Mutter & Cande, 1983). Simultaneously, long-term volcanism at the nearby Northern Kerguelen Plateau started (Coffin et al., 2002; Doucet et al., 2002; Duncan, 2002; Nicolaysen et al., 2000; Weis & Frey, 2002) and has continued until the present day, as evidenced by active fumaroles at the Kerguelen Archipelago (Patrick & Smellie, 2013). The current hotspot location is, however, debatable, since the neighboring Central Kerguelen Plateau has also been volcanically active over the past 22 Ma (Weis et al., 2002; Duncan et al., 2016) and eruptions have recently been monitored at Heard and McDonald Island (Patrick & Smellie, 2013).

Regarding the plume history, it should be noted that the Kerguelen Plateau has been generated in three clearly distinct periods of plume activity, even though its structure appears to be continuous on topographic maps. Also, split in three distinct parts is the Kerguelen hotspot track reconstructed in the Doubrovine et al. (2012) mantle reference frame (see Figure 1). It demonstrates that the Kerguelen plume has successively affected the Indian, Australian, and Antarctic Plates and even simultaneously at times when the plume was close enough to interact with a spreading ridge. The long-term proximity and interaction of the Kerguelen plume and the plate boundaries in the Indian Ocean has been validated by the plate tectonic models of Whittaker et al. (2013, 2015).

Another region relevant to the Kerguelen plume history is the volcanically active Amsterdam-Saint Paul Plateau (Johnson et al., 2000), which is located ~1,400 km northeast of the Kerguelen Archipelago and situated directly on the axis of the Southeast Indian Ridge. This plateau has been created during the past 10 Myr, and the Chain of the Dead Poets is regarded as its corresponding hotspot track that was formed over the past 20 Myr and trends age-progressively from the southern end of the Ninetyeast Ridge toward the Amsterdam-Saint Paul Plateau (Janin et al., 2011; Maia et al., 2011). Already, Morgan (1978) suggested that this region might be fed by the Kerguelen plume through an asthenospheric flow channel, a hypothesis that was supported by the flow models of Yale and Morgan (1998). Geochemical studies have, however, shown that the isotopic compositions from Amsterdam and Saint Paul Island, nearby ridge segments, and an active submarine volcano are (apart from being clearly distinct from each other) incompatible with the characteristics of Kerguelen plume material and therefore regard the Amsterdam-Saint Paul plume as a second, independent plume with indications of a deep source (Doucet et al., 2004; Graham et al., 1999; Johnson et al., 2000; Nicolaysen et al., 2007).

Altogether, it can be summarized that the geodynamic history of the Kerguelen plume and its magmatic output is very complex and challenges the classical plume model (e.g., Courtillot et al., 2003) as well as other characteristics potentially linked to plumes (e.g., Coffin & Eldholm, 1992; Courtillot et al., 1999) in different ways: the first eruptions produced only small volumes of basalt; the LIP was created long after the continental breakup; when the large-volume output finally started, it continued for an unusually long period; many different distinct provinces were affected by the plume, and currently, a second deeply rooted plume might be situated not too far away. Despite the remote location of most parts of this area, it was the destination of various ocean drilling expeditions and most of the abundant published studies focussed on gaining further insights for the reconstruction of the origin and evolution of the Kerguelen plume history. Our study, however, provides the first geodynamic model of the Kerguelen plume that explicitly considers its local surroundings and a realistic plate tectonic geometry over time. The results can therefore be compared to the existing age dates, the structures of the igneous provinces, and estimates of the crustal thickness and the melt production rate. Most importantly, the dynamic behavior of the model reveals new perspectives on the apparent inconsistencies with the plume characteristics listed above.

2. Model Setup

Following the methods described in detail in Gassmöller et al. (2016) and Bredow et al. (2017), we set up a regional viscous flow model with the mantle convection code ASPECT (Bangerth et al., 2017; Heister et al., 2017) in order to explore the geodynamic history of the Kerguelen hotspot.

The model domain is a 3,300 km long, 3,300 km wide, and 660 km high Cartesian box that specifically simulates the surrounding conditions of the Kerguelen plume by combining various initial and time-dependent boundary conditions.

Reconstructed plate boundaries (interpolations of Torsvik et al., 2010) and plate velocities are prescribed on top of the box and the uppermost 200 km of the side boundaries (based on the reference frame of Doubrovine et al., 2012).

Large-scale global mantle flow velocities are prescribed at depths greater than 200 km at the side boundaries and the bottom of the box. They are derived from a lower resolved global convection model (an update of Doubrovine et al., 2012), which is based on a superposition of plate-driven flow and density-driven flow. Density anomalies for the second component are computed by backward advecting present-day density heterogeneities from the SMEAN tomography model of Becker and Boschi (2002) but only back to 68 Ma, because the neglect of diffusion makes the backward advection procedure increasingly inappropriate further back in time. The plate-driven flow component is, however, fully time dependent, and therefore so are the global flow boundary conditions. For the model dynamics, a constant density-driven flow component corresponds to the assumption that the large-scale mantle structure — with upwellings above the two large low-shear velocity provinces and downwellings in regions where subduction has occurred — remained similar through the past 120 Myr.

Furthermore, an inhomogeneous lithosphere thickness pattern simulates the distribution of continental and oceanic lithosphere, implemented as temperature boundary conditions (backward rotations of the global lithosphere thickness model of (Steinberger, 2016), for continental areas; backward rotated ocean floor age of (Müller et al., 2008), converted to half-space cooling temperatures for oceanic areas and considering that the lithosphere cools and thickens with age).

Note that apart from the initial state of the model, all these conditions are only prescribed at the boundaries of the box, while the model development inside the box is completely dynamic. Thus, the model is able to show how the plume may have responded over time to nearby moving mid-ocean ridges and a variable lithosphere thickness pattern moving across the plume.

The viscosity in the model (equivalent to Bredow et al., 2017) is temperature dependent and depth dependent after Steinberger and Calderwood (2006) but also takes into account a dehydration rheology to consider the sudden viscosity increase due to the extraction of water from olivine during melting. Additionally, a depletion buoyancy induces a density decrease when melt is extracted.

Melting in the model depends on temperature and pressure, following the parametrization of Katz et al. (2003) for batch melting of anhydrous peridotite. In each time step, the generated melt is instantly extracted vertically upward to the surface and, in a postprocessing procedure, moved to the present-day location with the

according plate motions. The generated melt in its entirety finally shows the Kerguelen hotspot track as predicted by the model, that is, at which areas the plume may have produced a certain thickness of crust. To investigate the crustal thickness contribution of the plume alone, we have to correct for the melt generated along the spreading ridges from passively upwelling material, without any plume influence. Therefore, our results show the difference between the model with the plume as described in this section and another model with exactly the same setup but without a plume.

As shown in Bredow et al. (2017), our model setup is not designed to handle melting in continental environments with high lithosphere thickness values (such as eastern Gondwana before ~132 Ma). It also remains somewhat enigmatic as to what prevented the Kerguelen plume, if it already ponded underneath eastern Gondwana and produced the small-volume igneous provinces described above, from vigorous volcanic activities as soon as the Indian Ocean basin started to open and placed thin oceanic lithosphere above the plume. In this case, the Southern Kerguelen Plateau would have been created contiguously with the Antarctic continental margin, as already noted by Müller et al. (1993). Therefore, our model does not start until 120 Ma, and the plume head enters the model at that time with an excess temperature $\Delta T_{\mathrm{head}} = 300$ K, radius $R_{\mathrm{head}} = 250$ km, and a vertical inflow velocity $v_{\mathrm{head}} = 20$ cm/yr, corresponding to Bredow et al. (2017), such that the spatial extent of the melting region agrees approximately with the surface area of the Southern and Central Kerguelen Plateau. Thus, first plume-derived melts are generated at 118.75 Ma, in agreement with the onset of melting at the Southern Kerguelen Plateau (circa 120–110 Ma; Coffin et al., 2002; Duncan, 2002) and the Rajmahal Traps (118–115 Ma; Baksi, 1995; Coffin et al., 2002; Kent et al., 2002) and Sylhet Traps (118–116 Ma; Ghatak & Basu, 2011; Ray et al., 2005).

For the plume tail, excess temperature estimates range between 209 and 232 K (Putirka, 2008; Schilling, 1991) and buoyancy flux estimates range between 200 and 2,070 kg/s (Davies, 1988; Schilling, 1991; Sleep, 1990; Turcotte & Schubert, 2002). In our model, $\Delta T_{\mathrm{tail}} = 250$ K, $R_{\mathrm{tail}} = 140$ km, and $v_{\mathrm{tail}} = 6$ cm/yr. The prescribed excess temperature is higher than the published values, because it decreases during its ascent from the bottom of the box to the melting area, where it arrives with an excess temperature within the estimated range. The buoyancy flux of the plume at the bottom of the box yields approximately 1,150 kg/s, in the midst of the range of published estimates. We use a plume inflow position that is fixed in the global moving hotspot reference frame of Doubrovine et al. (2012) underneath the present location of the Kerguelen Archipelago, because Steinberger (2000) reported the best fit for a fixed plume. Note that since Kerguelen was not one of the plumes used to devise the Doubrovine et al. (2012) frame, assuming a fixed plume is not self-contradictory. To prevent any net mass influx or outflux of the model domain and especially balance the plume inflow, each model runs a second time with velocity boundary conditions that are corrected with the net mass flux derived from the first model run (see Gassmöller et al., 2016, for details).

3. Results

The model results are visualized in Figure 2: the large map on the right shows the entire crustal thickness pattern produced by the modeled plume to be compared to the topographic structures. To identify when each part of the hotspot track was created, the total result has been split into partial results for 10 Myr intervals, plotted on the smaller topographic maps. The evolution of the plume and its interaction with nearby spreading ridges can be followed along the interval maps and the inset figures, showing top views of the model at the respective times. For a description of tested parameter variations and how they affect the model results, see supporting information Text S1.

At 115 Ma, the plume head has reached the surface underneath the nascent Indian Ocean between India and Antarctica. The thin oceanic lithosphere and the dimension of the plume head enable extensive melting on both the Antarctic and the Indian Plates, and this results in the formation of the Southern Kerguelen Plateau, although shifted to the east in comparison to the present-day topography, and the Rajmahal and Sylhet Traps, shifted to the southeast (see black arrows). Some melt is also generated close to the Naturaliste, Wallaby, and Zenith Plateaus but not on the Gulden Draak Knoll (117 Ma) and there is no melt at all close to the lamprophyres at Antarctica (114 Ma). The timing for the origin of the Rajmahal Traps (118–115 Ma) and Sylhet Traps (118–116 Ma) and the Southern Kerguelen Plateau (120–110 Ma), however, is exactly reproduced in the model, due to the chosen initiation time of the modeled plume (see section 1 for age references).

Between 110 and 100 Ma, most of the crust is produced at the fast-moving Antarctic plate, creating the Central Kerguelen Plateau in agreement with age dates (105–100 Ma), whereas only little crust is produced

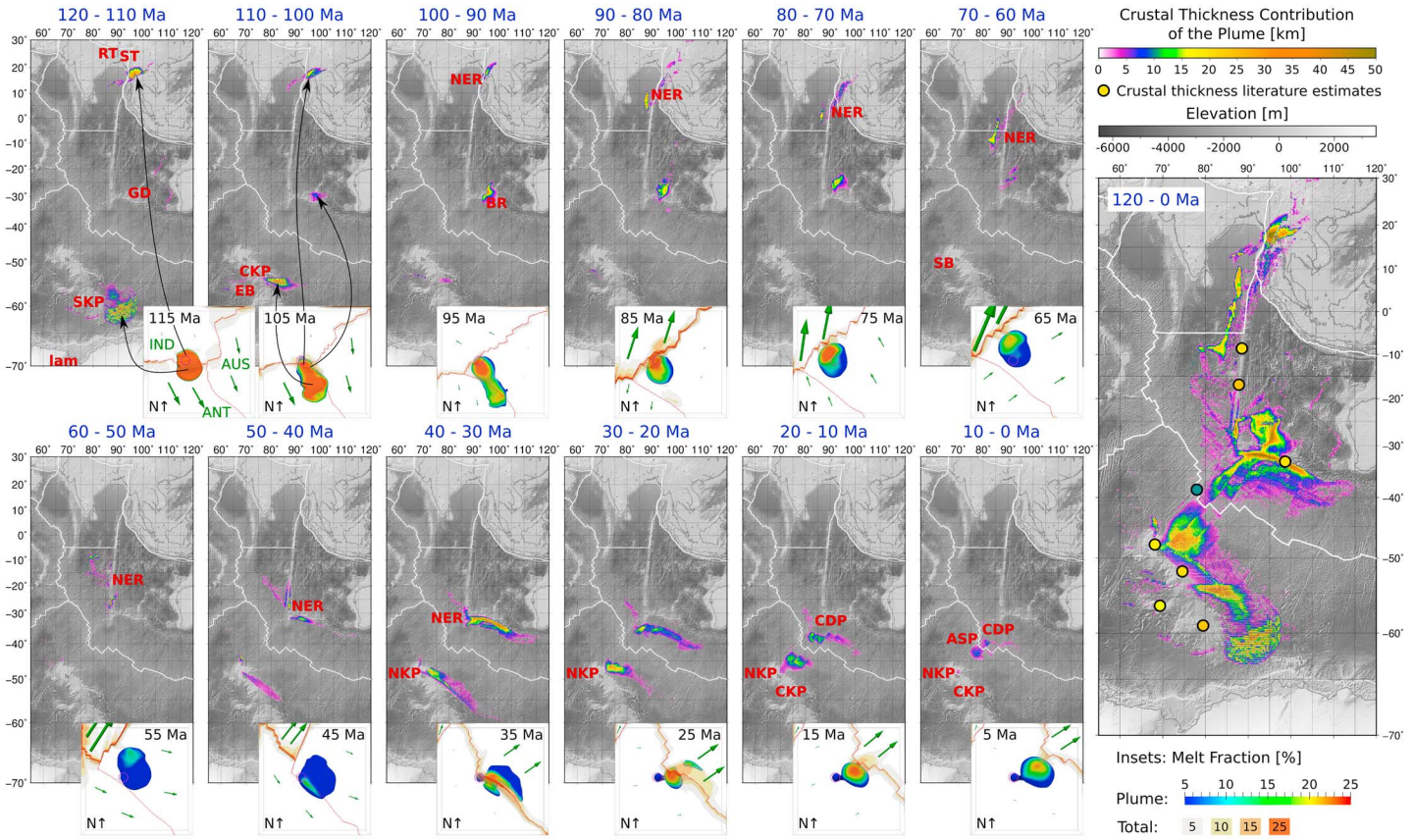

Figure 2. Large map: crustal thickness pattern predicted by the modeled plume over the past 120 Ma, where color-coded circles correspond to literature estimates. Smaller maps: predicted crustal thickness pattern divided into 10 Myr intervals, plotted with present-day plate boundaries and red labels indicating approximately the areas in which igneous material was created during this interval (for abbreviations, see Figure 1). Insets show top views of the model in the middle of each respective time interval, where plate boundaries (in red) correspond to the respective time. The plume is visualized by the 100 K excess temperature isocontour and colored according to the melt fraction. Isocontours show total melt fractions above 5% in the entire model domain. Green arrows depict the plate velocities, and the pink circles indicate the position of the plume stem at the bottom of the model box (apparent shift due to 3-D view from vertically above the center of the model, not vertically above the plume).

at Elan Bank (110–105 Ma). Around 105 Ma, the plume interacts with the triple junction between the Indian, Australian, and Antarctic plates, thus generating crust at three different plates at the same time.

At 95 Ma, the plume is mostly situated underneath the Australian plate and creates the Broken Ridge (95–94 Ma), matching age dates very well. Subsequently, the Indian Plate accelerates to its record velocities before the collision with the Eurasian plate, and plume material gets captured by the ridge between India and Australia. This marks the onset of long-term decompression melting along the ridge that generates the Ninetyeast Ridge (82–37 Ma), including the part presumably covered underneath the Bengal Fan (95–85 Ma). This is a surprising and novel result, because many previous studies (e.g., Duncan, 1991; Duncan & Richards, 1991) agreed that the Ninetyeast Ridge results from the Indian Plate moving above the Kerguelen plume—yet in our model, the plume is located underneath the Australian plate between 95 and 45 Ma and the Ninetyeast Ridge is clearly produced on the ridge axis and not directly above the plume.

The opening of the Southeast Indian Ridge at 40 Ma results in a period of intensive on-ridge volcanism that starts to form the Northern Kerguelen Plateau at the Antarctic plate around 40 Ma, matching age dates excellently. The large-scale structure on the conjugate Australian plate resembles the Broken Ridge very well, but it is much younger than indicated by oceanic drilling (95–94 Ma).

Approaching the present-day model state, there is no crust generated at the Central Kerguelen Plateau, but on the Northern Kerguelen Plateau melting occurs close to the Kerguelen Archipelago. Another interesting result concerns the Amsterdam-Saint Paul Plateau: in agreement with age dates, crust is generated close to the Chain of the Dead Poets over the past 20 Ma, and currently, the model predicts crustal material also close

to the ridge, in the vicinity of the Amsterdam-Saint Paul Plateau. The inset map reveals that the plume has a circular shape at 5 Ma, which means that it is no longer captured by the ridge, and intraplate volcanism creates the melt at the Kerguelen Plateau. However, there is still a flow connection which transports plume material toward the ridge (in agreement with Morgan, 1978; Yale & Morgan, 1998) and the crust close to the Amsterdam-Saint Paul Plateau is the product of on-ridge volcanism. Even though geochemical studies conclude differently, our model provides a simple yet elegant explanation for the observed volcanic structures without the need for a second plume.

All in all, the crustal thickness pattern predicted by the model over the past 120 Ma (large map on the right) resembles the topographic structures associated with Kerguelen plume activities remarkably well. The Ninetyeast Ridge, although shifted to the west and not entirely continuous (due to the decreasing amount of spreading segments at the Indian-Australian plate boundary, where most melt is generated), is clearly recognizable, as well as the Broken Ridge. The Kerguelen Plateau is predicted to result explicitly from three distinct periods of volcanism, although shifted to the east in the model relative to its true location. Apart from several small-scale areas, where the model reaches maximum crustal thickness values of about 45 km, the model result approximately fits the range of literature values from seismic refraction and reflection studies, wide-angle seismic data, gravity, bathymetry, and isostasy analyses (marked by color-coded filled circles on the map): 21–25 km at the Southern Kerguelen Plateau (Operto & Charvis, 1995, 1996), 19–21 km at the Central Kerguelen Plateau (Charvis et al., 1995), at least 16 km at Elan Bank (Borissova et al., 2003), circa 22–24 km at the Ninetyeast Ridge (Grevemeyer et al., 2001; Krishna et al., 2001), 18–22 km at the Broken Ridge (Francis & Raitt, 1967), 15–21 km at the Northern Kerguelen Plateau and Archipelago (Charvis et al., 1995; Recq et al., 1990), and 10 km on average at the Amsterdam-Saint Paul Plateau (Scheirer et al., 2000). It must, however, be considered that a direct comparison is not entirely accurate, since the modeled crustal thickness is only accumulated by plume activities, whereas the contribution of melting along the spreading ridges is removed from the model result.

Based on radiometric age determinations and crustal structure volume estimates, Coffin et al. (2002) calculated the magmatic output rate of the Kerguelen plume over time and concluded that the melt production rate has been substantially variable (see Figure 3a), with a discontinuous 25 Myr peak magma output. To account for these results, Coffin et al. (2002) suggested the involvement of multiple plumes or one plume split into several diapirs by vigorous mantle shear flow. Based on numerical models of thermal plumes, Lin and van Keken (2005) demonstrated that the entrainment of dense material in the lowermost mantle can lead to multiple pulses of plume material and thus be another explanation for several volcanic episodes generating flood basalts. Sreejith and Krishna (2015) reported a rapidly varying magma production rate along the Ninetyeast Ridge (see Figure 3a) and attributed the long-term variations to the frequent ridge jumps and major velocity changes of the Indian Plate, whereas short-term variations were explained by solitary waves in the plume tail. Referring to these results, Figure 3b shows the magma production rate in the model, derived both for the 10 Ma intervals as shown in Figure 2 and also for 1 Ma intervals in order to visualize the short-term variations. Note that due to an applied smoothing algorithm, the 1 Ma intervals underestimate the magma flux by ~8%. The peak produced by the impact of the plume head reaches 0.9 km^3/yr, matching the rate estimated by Coffin et al. (2002), but it lasts only for a few million years in agreement with the classical plume model. Subsequently, the magma flux fluctuates significantly and reaches a second peak after the onset of spreading at the South East Indian Ridge at 40 Ma. Our model does not reach the values of Sreejith and Krishna (2015) during the creation of the Ninetyeast Ridge, but the total magma production of our model yields a volume of 1.98×10^7 km^3, comparable to the 2.5×10^7 km^3 given by Coffin et al. (2002). The reason for the fluctuations can best be seen by comparing the colors of the plume in the insets in Figure 2, which correspond to the degree of melting in the model. Even though the plume tail influx at the bottom of the model is constant, the melt production rate changes significantly over time, mainly influenced by the distance to mid-ocean ridges (which determines the thickness of the lithosphere the plume material impinges on), as well as the directions and velocities of nearby plate motions. Since all these influencing factors, in short, plume-ridge interaction, change considerably over time, the variable melt production rate is rather the direct consequence of a very dynamic long-term plume history than an indication of highly complicated plume properties—the main result of this study.

Returning to the unusual plume characteristics described in section 1, the model can explain neither why the oldest continental igneous provinces have very small volumes nor why the LIP significantly postdated the continental breakup. However, we show that the large-volume output does not have to continue for an

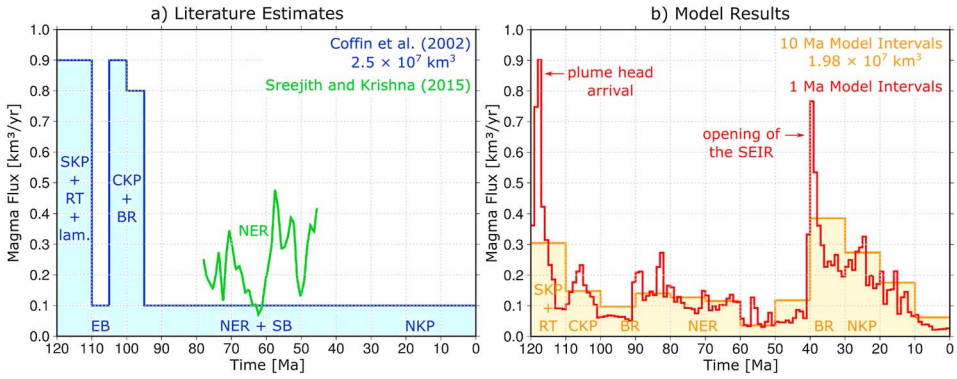

Figure 3. Variations in the melt production rate of the Kerguelen plume as (a) estimated by previous studies and (b) predicted by the model. All rates refer only to the excess of the normal oceanic crustal production. For abbreviations, see Figure 1.

uncommonly long period in order to create the observable topography structures. Furthermore, our model demonstrates that a single, not unusually buoyant or hot plume can cause the variety of widespread basaltic provinces attributed to Kerguelen plume activities as well as the current eruption sites at the Amsterdam-Saint Paul Plateau.

4. Conclusions

Our three-dimensional regional convection model of the Kerguelen mantle plume predicts the amount and distribution of plume-generated crust over the past 120 Ma. We compare the result to present-day topographic structures to gain insights into the geodynamic processes involved in the history of the plume, which leads to the following conclusions:

1. A constant plume influx can result in a significantly variable magma production rate due to the interaction of the plume with nearby mid-ocean ridges and plate motions.
2. The model indicates that the Ninetyeast Ridge was created by volcanism along the ridge axis between the Indian and Australian Plates, while the Kerguelen plume was located farther away underneath the Australian plate. This differs with previous studies that described the Ninetyeast Ridge as the result of the Indian Plate moving above the plume.
3. In a dynamic sense, the model suggests that the Amsterdam-Saint Paul Plateau is generated by volcanic material that flows from the plume conduit toward the axis of the Southeast Indian Ridge and leads to on-ridge eruptions, whereas the volcanic activities at the Kerguelen Plateau can be attributed to intraplate volcanism, directly above the plume.

Acknowledgments
This project is funded by the Deutsche Forschungsgemeinschaft (DFG) under grant STE 907/11-1 to B. S., and the computational resources were provided by the North-German Supercomputing Alliance (HLRN) as part of project bbp00006. The geodynamic models were computed with the open-source software ASPECT (https://aspect.geodynamics.org/), and the necessary data to reproduce the models are included in the supporting information. We thank Anneke Veting for helping to prepare the plate reconstructions used as boundary conditions, Simon Williams for inspiration at the right time, and Juliane Dannberg for helpful comments on the manuscript. We also thank Garrett Ito and Mike Coffin for constructive comments on the paper.

References

Antretter, M., Steinberger, B., Heider, F., & Soffel, H. (2002). Paleolatitudes of the Kerguelen hotspot: New paleomagnetic results and dynamic modeling. *Earth and Planetary Science Letters*, *203*(2), 635–650. https://doi.org/10.1016/S0012-821X(02)00841-5

Baksi, A. K. (1995). Petrogenesis and timing of volcanism in the Rajmahal flood basalt province, northeastern India. *Chemical Geology*, *121*(1), 73–90. https://doi.org/10.1016/0009-2541(94)00124-Q

Bangerth, W., Dannberg, J., Gassmöller, R., Heister, T., & others (2017). *ASPECT: Advanced Solver for Problems in Earth's ConvecTion, user manual*. https://doi.org/10.6084/m9.figshare.4865333

Becker, T. W., & Boschi, L. (2002). A comparison of tomographic and geodynamic mantle models. *Geochemistry, Geophysics, Geosystems*, *3*, 1003. https://doi.org/10.1029/2001GC000168

Borissova, I., Coffin, M. F., Charvis, P., & Operto, S. (2003). Structure and development of a microcontinent: Elan Bank in the southern Indian Ocean. *Geochemistry, Geophysics, Geosystems*, *4*(9), 1071. https://doi.org/10.1029/2003GC000535

Bredow, E., Steinberger, B., Gassmöller, R., & Dannberg, J. (2017). How plume-ridge interaction shapes the crustal thickness pattern of the Réunion hotspot track. *Geochemistry, Geophysics, Geosystems*, *18*(8), 2930–2948. https://doi.org/10.1002/2017GC006875

Bryan, S. E., & Ernst, R. E. (2008). Revised definition of Large Igneous Provinces (LIPs). *Earth-Science Reviews*, *86*(1), 175–202. https://doi.org/10.1016/j.earscirev.2007.08.008

Charvis, P., Recq, M., Operto, S., & Brefort, D. (1995). Deep structure of the northern Kerguelen Plateau and hotspot-related activity. *Geophysical Journal International*, *122*(3), 899–924. https://doi.org/10.1111/j.1365-246X.1995.tb06845.x

Coffin, M. F., & Eldholm, O. (1992). Volcanism and continental break-up: A global compilation of Large Igneous Provinces. *Geological Society, London, Special Publications*, *68*(1), 17–30. https://doi.org/10.1144/GSL.SP.1992.068.01.02

Coffin, M. F., & Eldholm, O. (1994). Large Igneous Provinces: Crustal structure, dimensions, and external consequences. *Reviews of Geophysics*, *32*(1), 1–36. https://doi.org/10.1029/93RG02508

Coffin, M. F., Pringle, M., Duncan, R., Gladczenko, T., Storey, M., Müller, R., & Gahagan, L. (2002). Kerguelen hotspot magma output since 130 Ma. *Journal of Petrology*, *43*(7), 1121–1137. https://doi.org/10.1093/petrology/43.7.1121

Courtillot, V., Davaille, A., Besse, J., & Stock, J. (2003). Three distinct types of hotspots in the Earth's mantle. *Earth and Planetary Science Letters*, *205*(3-4), 295–308. https://doi.org/10.1016/S0012-821X(02)01048-8

Courtillot, V., Jaupart, C., Manighetti, I., Tapponnier, P., & Besse, J. (1999). On causal links between flood basalts and continental breakup. *Earth and Planetary Science Letters*, *166*(3), 177–195. https://doi.org/10.1016/S0012-821X(98)00282-9

Davies, G. F. (1988). Ocean bathymetry and mantle convection: 1. Large-scale flow and hotspots. *Journal of Geophysical Research*, *93*, 10,467–10,480. https://doi.org/10.1029/JB093iB09p10467

Direen, N. G., Cohen, B. E., Maas, R., Frey, F. A., Whittaker, J. M., Coffin, M. F., ... Crawford, A. J. (2017). Naturaliste plateau: Constraints on the timing and evolution of the Kerguelen Large Igneous Province and its role in Gondwana breakup. *Australian Journal of Earth Sciences*, *64*(7), 1–19. https://doi.org/10.1080/08120099.2017.1367326

Domeier, M., & Torsvik, T. H. (2014). Plate tectonics in the late Paleozoic. *Geoscience Frontiers*, *5*(3), 303–350. https://doi.org/10.1016/j.gsf.2014.01.002

Doubrovine, P. V., Steinberger, B., & Torsvik, T. H. (2012). Absolute plate motions in a reference frame defined by moving hot spots in the Pacific, Atlantic, and Indian Oceans. *Journal of Geophysical Research*, *117*, B09101. https://doi.org/10.1029/2011JB009072

Doucet, S., Weis, D., Scoates, J. S., Debaille, V., & Giret, A. (2004). Geochemical and Hf-Pb-Sr-Nd isotopic constraints on the origin of the Amsterdam-St. Paul (Indian Ocean) hotspot basalts. *Earth and Planetary Science Letters*, *218*(1-2), 179–195. https://doi.org/10.1016/S0012-821X(03)00636-8

Doucet, S., Weis, D., Scoates, J. S., Nicolaysen, K., Frey, F. A., & Giret, A. (2002). The depleted mantle component in Kerguelen Archipelago basalts: Petrogenesis of tholeiitic-transitional basalts from the Loranchet Peninsula. *Journal of Petrology*, *43*(7), 1341–1366. https://doi.org/10.1093/petrology/43.7.1341

Duncan, R. A. (1991). Age distribution of volcanism along aseismic ridges in the eastern Indian Ocean. *Proceedings of the Ocean Drilling Program, Scientific Results*, *121*, 507–517. https://doi.org/10.2973/odp.proc.sr.121.162.1991

Duncan, R. A. (2002). A time frame for construction of the Kerguelen Plateau and Broken Ridge. *Journal of Petrology*, *43*(7), 1109–1119. https://doi.org/10.1093/petrology/43.7.1109

Duncan, R. A., Falloon, T. J., Quilty, P. G., & Coffin, M. F. (2016). Widespread Neogene volcanism on central Kerguelen Plateau, southern Indian Ocean. *Australian Journal of Earth Sciences*, *63*(4), 379–392. https://doi.org/10.1080/08120099.2016.1221857

Duncan, R. A., & Richards, M. A. (1991). Hotspots, mantle plumes, flood basalts, and true polar wander. *Reviews of Geophysics*, *29*(1), 31–50. https://doi.org/10.1029/90RG02372

Francis, T. J. G., & Raitt, R. W. (1967). Seismic refraction measurements in the southern Indian Ocean. *Journal of Geophysical Research*, *72*(12), 3015–3041. https://doi.org/10.1029/JZ072i012p03015

Frey, F., Coffin, M., Wallace, P., Weis, D., Zhao, X., Wise, S., ... Antretter, M. (2000). Origin and evolution of a submarine Large Igneous Province: The Kerguelen Plateau and Broken Ridge, southern Indian Ocean. *Earth and Planetary Science Letters*, *176*(1), 73–89. https://doi.org/10.1016/S0012-821X(99)00315-5

Frey, F. A., McNaughton, N. J., Nelson, D. R., deLaeter, J. R., & Duncan, R. A. (1996). Petrogenesis of the Bunbury Basalt, Western Australia: Interaction between the Kerguelen plume and Gondwana lithosphere?*Earth and Planetary Science Letters*, *144*(1), 163–183. https://doi.org/10.1016/0012-821X(96)00150-1

Gaina, C., Müller, R., Brown, B., & Ishihara, T. (2003). Microcontinent formation around Australia. *Geological Society of America Special Papers*, *372*, 405–416.

Gaina, C., Müller, R. D., Brown, B., Ishihara, T., & Ivanov, S. (2007). Breakup and early seafloor spreading between India and Antarctica. *Geophysical Journal International*, *170*(1), 151–169. https://doi.org/10.1111/j.1365-246X.2007.03450.x

Gardner, R. L., Daczko, N. R., Halpin, J. A., & Whittaker, J. M. (2015). Discovery of a microcontinent (Gulden Draak Knoll) offshore Western Australia: Implications for East Gondwana reconstructions. *Gondwana Research*, *28*(3), 1019–1031. https://doi.org/10.1016/j.gr.2014.08.013

Gassmöller, R., Dannberg, J., Bredow, E., Steinberger, B., & Torsvik, T. H. (2016). Major influence of plume-ridge interaction, lithosphere thickness variations, and global mantle flow on hotspot volcanism—The example of Tristan. *Geochemistry, Geophysics, Geosystems*, *17*(4), 1454–1479. https://doi.org/10.1002/2015GC006177

Graham, D., Johnson, K., Priebe, L., & Lupton, J. (1999). Hotspot-ridge interaction along the Southeast Indian Ridge near Amsterdam and St. Paul Islands: Helium isotope evidence. *Earth and Planetary Science Letters*, *167*(3-4), 297–310. https://doi.org/10.1016/S0012-821X(99)00030-8

Ghatak, A., & Basu, A. R. (2011). Vestiges of the Kerguelen plume in the Sylhet Traps, northeastern India. *Earth and Planetary Science Letters*, *308*(1), 52–64. https://doi.org/10.1016/j.epsl.2011.05.023

Grevemeyer, I., Flueh, E. R., Reichert, C., Bialas, J., Kläschen, D., & Kopp, C. (2001). Crustal architecture and deep structure of the Ninetyeast Ridge hotspot trail from active-source ocean bottom seismology. *Geophysical Journal International*, *144*(2), 414–431. https://doi.org/10.1046/j.0956-540X.2000.01334.x

Heister, T., Dannberg, J., Gassmöller, R., & Bangerth, W. (2017). High accuracy mantle convection simulation through modern numerical methods. II: Realistic models and problems. *Geophysical Journal International*, *210*(2), 833–851. https://doi.org/10.1093/gji/ggx195

Ingle, S., Weis, D., & Frey, F. A. (2002). Indian continental crust recovered from Elan Bank, Kerguelen Plateau (ODP Leg 183, Site 1137). *Journal of Petrology*, *43*(7), 1241–1257. https://doi.org/10.1093/petrology/43.7.1241

Janin, M., Hémond, C., Guillou, H., Maia, M., Johnson, K. T. M., Bollinger, C., ... Mudholkar, A. (2011). Hot spot activity and tectonic settings near Amsterdam-St. Paul Plateau (Indian Ocean). *Journal of Geophysical Research*, *116*, B05206. https://doi.org/10.1029/2010JB007800

Johnson, K., Graham, D., Rubin, K., Nicolaysen, K., Scheirer, D., Forsyth, D., ... Douglas-Priebe, L. (2000). Boomerang Seamount: The active expression of the Amsterdam-St. Paul hotspot, Southeast Indian Ridge. *Earth and Planetary Science Letters*, *183*(1-2), 245–259. https://doi.org/10.1016/S0012-821X(00)00279-X

Katz, R. F., Spiegelman, M., & Langmuir, C. H. (2003). A new parameterization of hydrous mantle melting. *Geochemistry, Geophysics, Geosystems*, *4*(9), 1073. https://doi.org/10.1029/2002GC000433

Kent, R. W., Pringle, M. S., Müller, R. D., Saunders, A. D., & Ghose, N. C. (2002). $^{40}Ar/^{39}Ar$ geochronology of the Rajmahal Basalts, India, and their relationship to the Kerguelen Plateau. *Journal of Petrology*, *43*(7), 1141–1153. https://doi.org/10.1093/petrology/43.7.1141

Krishna, K. S., Neprochnov, Y. P., Rao, D. G., & Grinko, B. N. (2001). Crustal structure and tectonics of the Ninetyeast Ridge from seismic and gravity studies. *Tectonics*, *20*(3), 416–433. https://doi.org/10.1029/2001TC900004

Lin, S.-C., & van Keken, P. E. (2005). Multiple volcanic episodes of flood basalts caused by thermochemical mantle plumes. *Nature*, *436*(7048), 250–252. https://doi.org/10.1038/nature03697

Liu, Z., Zhou, Q., Lai, Y., Qing, C., Li, Y., Wu, J., & Xia, X. (2015). Petrogenesis of the Early Cretaceous Laguila bimodal intrusive rocks from the Tethyan Himalaya: Implications for the break-up of eastern Gondwana. *Lithos*, *236*, 190–202. https://doi.org/10.1016/j.lithos.2015.09.006

Mahoney, J., Macdougall, J., Lugmair, G., & Gopalan, K. (1983). Kerguelen hotspot source for Rajmahal Traps and Ninetyeast Ridge? *Nature*, *303*, 385–389. https://doi.org/doi:10.1038/303385a0

Maia, M., Pessanha, I., Courrèges, E., Patriat, M., Gente, P., Hémond, C., ... Vatteville, J. (2011). Building of the Amsterdam-Saint Paul Plateau: A 10 Myr history of a ridge-hot spot interaction and variations in the strength of the hot spot source. *Journal of Geophysical Research*, *116*(B9), B09104. https://doi.org/10.1029/2010JB007768

Matthews, K. J., Maloney, K. T., Zahirovic, S., Williams, S. E., Seton, M., & Müller, R. D. (2016). Global plate boundary evolution and kinematics since the late Paleozoic. *Global and Planetary Change*, *146*, 226–250. https://doi.org/10.1016/j.gloplacha.2016.10.002

Morgan, W. J. (1978). Rodriguez, Darwin, Amsterdam, … , A second type of Hotspot Island. *Journal of Geophysical Research*, *83*(B11), 5355–5360. https://doi.org/10.1029/JB083iB11p05355

Müller, R. D., Royer, J.-Y., & Lawver, L. A. (1993). Revised plate motions relative to the hotspots from combined Atlantic and Indian Ocean hotspot tracks. *Geology*, *21*(3), 275. https://doi.org/10.1130/0091-7613(1993)021<0275:RPMRTT>2.3.CO;2

Müller, R. D., Sdrolias, M., Gaina, C., & Roest, W. R. (2008). Age, spreading rates, and spreading asymmetry of the world's ocean crust. *Geochemistry, Geophysics, Geosystems*, *9*, Q04006. https://doi.org/10.1029/2007GC001743

Müller, R. D., Seton, M., Zahirovic, S., Williams, S. E., Matthews, K. J., Wright, N. M., ... Cannon, J. (2016). Ocean basin evolution and global-scale plate reorganization events since Pangea breakup. *Annual Review of Earth and Planetary Sciences*, *44*(1), 107–138. https://doi.org/10.1146/annurev-earth-060115-012211

Mutter, J. C., & Cande, S. C. (1983). The early opening between Broken Ridge and Kerguelen Plateau. *Earth and Planetary Science Letters*, *65*(2), 369–376. https://doi.org/10.1016/0012-821X(83)90174-7

Nicolaysen, K., Bowring, S., Frey, F., Weis, D., Ingle, S., Pringle, M. S., & Coffin, M. F. (2001). Provenance of Proterozoic garnet-biotite gneiss recovered from Elan Bank, Kerguelen Plateau, southern Indian Ocean. *Geology*, *29*(3), 235. https://doi.org/10.1130/0091-7613(2001)029<0235:POPGBG>2.0.CO;2

Nicolaysen, K., Frey, F., Hodges, K., Weis, D., & Giret, A. (2000). $^{40}Ar/^{39}Ar$ geochronology of flood basalts from the Kerguelen Archipelago, southern Indian Ocean: Implications for Cenozoic eruption rates of the Kerguelen plume. *Earth and Planetary Science Letters*, *174*(3–4), 313–328. https://doi.org/10.1016/S0012-821X(99)00271-X

Nicolaysen, K. P., Frey, F. A., Mahoney, J. J., Johnson, K. T. M., & Graham, D. W. (2007). Influence of the Amsterdam/St. Paul hot spot along the Southeast Indian Ridge between 77° and 88°E: Correlations of Sr, Nd, Pb, and He isotopic variations with ridge segmentation. *Geochemistry, Geophysics, Geosystems*, *8*(9), Q09007. https://doi.org/10.1029/2006GC001540

Olierook, H. K., Jourdan, F., Merle, R. E., Timms, N. E., Kusznir, N., & Muhling, J. R. (2016). Bunbury Basalt: Gondwana breakup products or earliest vestiges of the Kerguelen mantle plume?*Earth and Planetary Science Letters*, *440*, 20–32. https://doi.org/10.1016/j.epsl.2016.02.008

Olierook, H. K., Merle, R. E., & Jourdan, F. (2017). Toward a greater Kerguelen Large Igneous Province: Evolving mantle source contributions in and around the Indian Ocean. *Lithos*, *282*, 163–172. https://doi.org/10.1016/j.lithos.2017.03.007

Olierook, H. K., Merle, R. E., Jourdan, F., Sircombe, K., Fraser, G., Timms, N. E., ... Borissova, I. (2015). Age and geochemistry of magmatism on the oceanic Wallaby Plateau and implications for the opening of the Indian Ocean. *Geology*, *43*(11), 971. https://doi.org/10.1130/G37044.1

O'Neill, C., Müller, D., & Steinberger, B. (2003). Geodynamic implications of moving Indian Ocean hotspots. *Earth and Planetary Science Letters*, *215*(1), 151–168. https://doi.org/10.1016/S0012-821X(03)00368-6

Operto, S., & Charvis, P. (1995). Kerguelen Plateau: A volcanic passive margin fragment?*Geology*, *23*(2), 137–140. https://doi.org/10.1130/0091-7613(1995)023<0137:KPAVPM>2.3.CO;2

Operto, S., & Charvis, P. (1996). Deep structure of the southern Kerguelen Plateau (southern Indian Ocean) from ocean bottom seismometer wide-angle seismic data. *Journal of Geophysical Research*, *101*(B11), 25,077–25,103. https://doi.org/10.1029/96JB01758

Patrick, M. R., & Smellie, J. L. (2013). Synthesis: A spaceborne inventory of volcanic activity in Antarctica and southern oceans, 2000–10. *Antarctic Science*, *25*(4), 475–500. https://doi.org/10.1017/S0954102013000436

Powell, C., Roots, S., & Veevers, J. (1988). Pre-breakup continental extension in east Gondwanaland and the early opening of the eastern Indian Ocean. *Tectonophysics*, *155*(1), 261–283. https://doi.org/10.1016/0040-1951(88)90269-7

Putirka, K. (2008). Excess temperatures at ocean islands: Implications for mantle layering and convection. *Geology*, *36*(4), 283–286. https://doi.org/10.1130/G24615A.1

Ray, J. S., Pattanayak, S. K., & Pande, K. (2005). Rapid emplacement of the Kerguelen plume-related Sylhet Traps, eastern India: Evidence from ^{40}Ar-^{39}Ar geochronology. *Geophysical Research Letters*, *32*, L10303. https://doi.org/10.1029/2005GL022586

Recq, M., Brefort, D., Malod, J., & Veinante, J.-L. (1990). The Kerguelen Isles (southern Indian Ocean): New results on deep structure from refraction profiles. *Tectonophysics*, *182*(3-4), 227–248. https://doi.org/10.1016/0040-1951(90)90165-5

Richards, M. A., Duncan, R. A., & Courtillot, V. E. (1989). Flood basalts and hot-spot tracks: Plume heads and tails. *Science*, *246*, 103–107. https://doi.org/10.1126/science.246.4926.103

Scheirer, D. S., Forsyth, D. W., Conder, J. A., Eberle, M. A., Hung, S.-H., Johnson, K. T. M., & Graham, D. W. (2000). Anomalous seafloor spreading of the Southeast Indian Ridge near the Amsterdam-St. Paul Plateau. *Journal of Geophysical Research*, *105*(B4), 8243–8262. https://doi.org/10.1029/1999JB900407

Schilling, J.-G. (1991). Fluxes and excess temperatures of mantle plumes inferred from their interaction with migrating mid-ocean ridges. *Nature*, *352*, 397–403. https://doi.org/10.1038/352397a0

Sleep, N. H. (1990). Hotspots and mantle plumes: Some phenomenology. *Journal of Geophysical Research*, *95*(B5), 6715–6736. https://doi.org/10.1029/JB095iB05p06715

Sreejith, K. M., & Krishna, K. S. (2015). Magma production rate along the Ninetyeast Ridge and its relationship to Indian Plate motion and Kerguelen hot spot activity. *Geophysical Research Letters*, *42*(4), 1105–1112. https://doi.org/10.1002/2014GL062993

Stagg, H. M. J., Colwell, J. B., Borissova, I., Ishihara, T., & Bernardel, G. (2006). The bruce rise area, east Antarctica: Formation of a continental margin near the greater India–Australia–Antarctica triple junction. *Terra Antartica*, *13*(1/2), 3–22.

Steinberger, B. (2000). Plumes in a convecting mantle: Models and observations for individual hotspots. *Journal of Geophysical Research*, *105*(B5), 11,127–11,152. https://doi.org/10.1029/1999JB900398

Steinberger, B. (2016). Topography caused by mantle density variations: Observation-based estimates and models derived from tomography and lithosphere thickness. *Geophysical Journal International*, *205*, 604–621. https://doi.org/10.1093/gji/ggw040

Steinberger, B., & Calderwood, A. R. (2006). Models of large-scale viscous flow in the Earth's mantle with constraints from mineral physics and surface observations. *Geophysical Journal International*, *167*(3), 1461–1481. https://doi.org/10.1111/j.1365-246X.2006.03131.x

Torsvik, T. H., Steinberger, B., Gurnis, M., & Gaina, C. (2010). Plate tectonics and net lithosphere rotation over the past 150 My. *Earth and Planetary Science Letters*, *291*, 106–112. https://doi.org/10.1016/j.epsl.2009.12.055

Turcotte, D. L., & Schubert, G. (2002). *Geodynamics* (2nd ed.), Cambridge: Cambridge University Press.
Weis, D., & Frey, F. A. (2002). Submarine basalts of the northern Kerguelen Plateau: Interaction between the Kerguelen plume and the southeast Indian Ridge revealed at ODP Site 1140. *Journal of Petrology*, *43*(7), 1287–1309. https://doi.org/10.1093/petrology/43.7.1287
Weis, D., Frey, F. A., Schlich, R., Schaming, M., Montigny, R., Damasceno, D., ... Scoates, J. S. (2002). Trace of the Kerguelen mantle plume: Evidence from seamounts between the Kerguelen Archipelago and Heard Island, Indian Ocean. *Geochemistry, Geophysics, Geosystems*, *3*(6), 1–27. https://doi.org/10.1029/2001GC000251
Weis, D., Ingle, S., Damasceno, D., Frey, F. A., Nicolaysen, K., Barling, J., & Party, L. . S. S. (2001). Origin of continental components in Indian Ocean basalts: Evidence from Elan Bank (Kerguelen Plateau, ODP Leg 183, Site 1137). *Geology*, *29*(2), 147–150. https://doi.org/10.1130/0091-7613(2001)029<0147:OOCCII>2.0.CO;2
Whittaker, J. M., Afonso, J., Masterton, S., Müller, R., Wessel, P., Williams, S., & Seton, M. (2015). Long-term interaction between mid-ocean ridges and mantle plumes. *Nature Geoscience*, *8*(6), 479–483. https://doi.org/10.1038/ngeo2437
Whittaker, J., Williams, S., Halpin, J., Wild, T., Stilwell, J., Jourdan, F., & Daczko, N. (2016). Eastern Indian Ocean microcontinent formation driven by plate motion changes. *Earth and Planetary Science Letters*, *454*, 203–212. https://doi.org/10.1016/j.epsl.2016.09.019
Whittaker, J. M., Williams, S. E., & Müller, R. D. (2013). Revised tectonic evolution of the eastern Indian Ocean. *Geochemistry, Geophysics, Geosystems*, *14*(6), 1891–1909. https://doi.org/10.1002/ggge.20120
Yale, M. M., & Morgan, J. P. (1998). Asthenosphere flow model of hotspot-ridge interactions: A comparison of Iceland and Kerguelen. *Earth and Planetary Science Letters*, *161*(1), 45–56. https://doi.org/10.1016/S0012-821X(98)00136-8
Zhu, D.-C., Chung, S.-L., Mo, X.-X., Zhao, Z.-D., Niu, Y., Song, B., & Yang, Y.-H. (2009). The 132 Ma Comei-Bunbury Large Igneous Province: Remnants identified in present-day southeastern Tibet and southwestern Australia. *Geology*, *37*(7), 583. https://doi.org/10.1130/G30001A.1
Zhu, D., Mo, X., Pan, G., Zhao, Z., Dong, G., Shi, Y., ... Zhou, C. (2008). Petrogenesis of the earliest Early Cretaceous mafic rocks from the Cona area of the eastern Tethyan Himalaya in south Tibet: Interaction between the incubating Kerguelen plume and the eastern Greater India lithosphere? *Lithos*, *100*(1), 147–173. https://doi.org/10.1016/j.lithos.2007.06.024